

A Comparative Study between Two Versions of Southern California Seismic Velocity Models: CVMS-4 and the latest one, CVM-SI.26, through Simulation and Validation of Multiple Historical Events

Ricardo Taborda,^{1,2*} Shima Azizzadeh-Roodpish,^{1,2} and Naeem Khoshnevis,²

¹ Department of Civil Engineering, University of Memphis, Memphis, TN 38152, USA

² Center for Earthquake Research and Information, University of Memphis, Memphis, TN 38152, USA

To be submitted by September, 2015

1 INTRODUCTION

Among the several alternatives to earthquake ground motion simulations, physics-based, deterministic approach have drawn significant attention from seismologists and earthquake engineers (e.g. Tromp et al. 2010; Aagaard et al. 2010; Graves et al. 2011; Isbiliroglu et al. 2015) specially due to the increasing capacity and availability of high-performance computer systems and applications (e.g. Cui et al. 2010) which make it possible now to have different seismic velocity models available for various regions such as southern and northern California in the United States (Kohler et al. 2003; Brocher et al. 2006); the Grenoble and Volvi valleys in Europe (Chaljub et al. 2010; Manakou et al. 2010); and Japan (Koketsu et al. 2008; Fujiwara et al. 2009).

Being able to develop models that can be applied more broadly, and that can be continuously updated by a community of users has became the point of interest in simulation-based hazard analysis which lead to making models known as community velocity models, or CVMs. Two series of CVM-S (Magistrale et al., 2000; Kohler et al., 2003), and CVM-H (Sss and Shaw, 2003) released by Southern California Earthquake Center (SCEC) are good examples of community models. They have evolved over time with contributions from a community of researchers who study the earthquake hazards and ground motion characteristics in southern California.

CVM-S, also known as CVM-S4, was originally developed by Magistrale et al. (1996) and later updated by Magistrale et al. (2000) and Kohler et al. (2003). Recently, a new version of CVM-S, called CVM-S4.26 was built based on the original model CVM-S4 and the results of a sequence of 3D full-waveform tomographic inversions done by Chen et al. (2007) and Lee et al. (2014b). CVM-S is known as an acceptable representations of the crustal structure in southern California, at low frequencies ($f \leq 0.2$ Hz) and also according to our current parallel research for evaluating that, even till 1 Hz frequency, it is getting better results than the alternative model CVM-H for the region. Those results are in agreement with previous works done in the area for particular cases (e.g. Taborda & Bielak (2014), Lee et al. (2014a)). There are currently three alternative CVM-SI.26 models (2.2.1, 2.2.2 & 2.2.3) which vary depending on how the perturbations were applied to the original model. The ability to properly simulate seismograms depends on the challenge of finding the most accurate models of 3D crustal structure. Different models can lead to significantly different results, even at very low frequencies (e.g. Lee et al. 2014a; Taborda & Bielak

2014). There have been some researches with the aim of evaluation of different velocity models for southern California region in lower frequencies or for limited number of events. Such differences, however, have never been studied extensively, in order to compare different available models at frequencies beyond the upper limits set by the underlying inversions used to construct the models.

So, here, we designed a procedure to evaluate the overall improvement of accuracy of this recent southern California velocity model, CVM-SI.26, in predicting ground motion of the region, through comparing the results from different versions of CVM-S. Four different version of seismic velocity model, including CVM-S4, CVM-SI26.2.2.1, CVM-SI26.2.2.2 & CVM-SI26.2.2.3, and a set of historical events, containing thirty moderate-magnitude earthquakes ($3.5 > M_w > 5.5$) are considered for conducting a systematic evaluation, using validation of multiple simulations, through quantitative comparisons between synthetics and data. Events occurred between 1998 and 2014 and their are spread throughout the region and within a simulation domain with a surface projection area of $180 \text{ km} \times 135 \text{ km}$. The simulations are performed using a finite element application for solving forward wave propagation problems due to kinematic faulting (Tu et al. 2006; Taborda et al. 2010), with a numerical model built to represent a maximum frequency, $f_{\max} = 1 \text{ Hz}$ and a minimum shear wave velocity, $V_{S,\min} = 200 \text{ m/s}$.

The comparisons between data and synthetics are ranked quantitatively by means of a goodness-of-fit (GOF) criteria obtained following a modified version of the criteria introduced by Anderson (2004). We compare the regional distribution of the GOF results for all events and all models, and draw conclusions from the results and how these correlate to the characteristics of the models. We find that, in light of our comparisons, one of the models consistently yields better results and explore the reasons leading to this conclusion which in addition to agreement with previous case studies by Taborda & Bielak (2014) and Lee et al. (2014a), shows that the improvements done to CVM-S based on the tomographic studies done by Chen et al. (2007) and Lee et al. (2014a) have positive effects at frequencies above the limit considered for the inversions (0.2 Hz).

2 DOMAIN AND MODELS

The simulation domain is a volume of size $180 \text{ km} \times 135 \text{ km} \times 62 \text{ km}$, which covers the entire Los Angeles metropolitan area and

most of the significant geologic structures around. (Fig. 1). The elastic properties (P - and S -wave velocities (V_P and V_S , respectively), and the material's density (ρ) of particles) within the simulation domain are determined based on the models CVM-S4, CVM-S4.26.2.2.1, CVM-S4.26.2.2.2, and CVM-S4.26.2.2.3 to be evaluated.

CVM-S4 was initially developed by Magistrale et al. (1996), and later improved by Magistrale et al. (2000) and Kohler et al. (2003). This model integrates available information about the major southern California basins using data from boreholes, oil-well samples, gravity observations, and seismic refraction surveys. The model in itself is built upon empirical rules that use the depths and ages estimated for a set of geological horizons calibrated for southern California. Below and outside the basins, CVM-S4 relies on the 3D seismic tomography model proposed by Hauksson (2000), and an upper-mantle model based on teleseismic inversions introduced into the model by Kohler et al. (2003).

CVM-S4.26, is a model recently developed by SCEC based on the results from a full 3D tomographic (F3DT) inversion done by Lee et al. (2014b). The inversion process involved a sequence of 26 iterations over a reference model extracted from CVM-S4, thus its name. This effort followed the procedure first applied to the Los Angeles region by Chen et al. (2007). In Lee et al. (2014b), the reference model corresponded to a regular grid of 500-m spacing in which the material properties extracted from CVM-S4 were truncated to minimum values of $V_P = 2000$ m/s, $V_S = 1000$ m/s and $\rho = 2000$ km/m³. The truncation was smoothed until the values extracted from the model reached 3000 m/s, 2000 m/s and 2300 km/m³, respectively. To compute the perturbations to the initial model, Lee et al. (2014b) used about 38,000 earthquake records and 12,000 ambient noise Green's functions, and combined two inversion methods, the adjoint-wavefield method (AW-F3DT; Tromp et al. 2005) and the scattering-integral method (SI-F3DT; Zhao et al. 2006). Each iteration in the procedure involved the computation of a forward simulation done using a staggered-grid finite-differences approach (Olsen 1994). The forward simulations were done for a maximum frequency, $f_{\max} = 0.2$ Hz; and the misfits were computed using seismograms band-pass filtered at 0.02–0.2 Hz. After the 26th iteration perturbations were obtained, the results were merged with the original CVM-S4 model using an interpolation scheme to recover the truncated values. This is the CVM-S4.26 model.

There are currently three alternative CVM-SI.26 models which vary depending on how the perturbations were applied to the original model. These models are:

(2.2.1) This model applies an integration scheme in which negative perturbations are only used outside the basins, and positive perturbations are used everywhere.

(2.2.2) This scheme applies negative perturbations only if outside the basins, and disregards positive perturbations when inside the basins.

(2.2.3) This scheme applies both negative and positive perturbations everywhere, but sets the original value inside the basins as a floor limit.

Basin refers to any structure with $V_s < 1000$ m/s adopting the cutoff value used by Lee et al. (2013) to build the starting model. In all cases, the schemes reverse the process used to build the starting model first, in order to recapture the original structures in CVM-S with values of $V_s < 1000$ m/s, and apply the perturbations later (as described). These schemes have been implemented in the SCEC Unified Community Velocity Model (UCVM) software framework (Gill et al. 2013), which has already been used to produce unstructured (etree) meshes (Taborda et al., 2007; Tu et al., 2003) at resolutions finer than that used in the inversion.

In all cases, we constructed rasterized versions of the models for the volume simulation domain shown in Fig. 1a. This was done using the Unified Community Velocity Model (UCVM) software framework developed by SCEC (Small et al. 2011; Gill et al. 2015), and the UCVM implementation of the etree library (Tu et al. 2003), which follows a similar procedure to that described in Taborda et al. (2007) and Schlosser et al. (2008).

Fig. 2 shows a comparison between the four models for the free-surface V_S and the depths to the isosurfaces at which V_S values reach 1.0 and 2.5 km/s. From the isosurfaces, Perhaps the larger contrasts between CVM-S4 and CVM-S4.26 are observed off shore and north of the San Andreas fault, in the Mojave desert (see Fig. 1 for reference). Other changes are observable in the Santa Clara river valley and Ventura basin, and in the vicinity of the San Bernardino basin, especially to the East (top-right corner of the simulation domain). In all these cases CVM-S4.26 exhibits deeper structures than CVM-S4. Most of the changes in CVM-S4.26 with respect to CVM-S4 are in the deeper structures, and to the north-west of the segment AB and to the east of segment BS.

3 EVENTS AND SOURCE PROPERTIES

The 30 earthquakes considered for the evaluation of the models in this article are labeled with a sequential letter-code from A to AD in Fig. 1 with their detailed information presented in Table 1 Lee et al. (2011). They are a set of earthquakes which are happened between 1998 and 2014, and had magnitudes between 3.6 and 5.4, and hypocenter depths that vary between 3.6 and 21.1 km. Events are modeled as a point source analogy with rupture parameters scaled according to the magnitude of each earthquake and source time functions respecting to that.

4 SIMULATION METHOD AND PARAMETERS

The simulation is done for each earthquake and velocity model using Hercules, a parallel 3D finite element computer application for solving forward anelastic wave propagation problems which has been thoroughly tested and verified in multiple supercomputers. It implements an octree datastructure for representing unstructured hexahedral meshes in memory (Tu et al. 2006) with a solution approach relies on a standard Galerkin method for discretizing the equations of elastodynamics in space, and advances explicitly in time to obtain the next-step state of nodal displacements.

Table 2 describes the main simulation parameters. All simulations were done on Blue Waters at the National Center for Supercomputing Applications. Table 2 also includes information about the average performance of the code for every simulation model. All simulations considered, we used over 0.27 million of CPU hours.

5 GROUND MOTION SIMULATION RESULTS

Before we address the evaluation of the models, we present results from the simulations and offer a general perspective on the ground motion characteristics obtained for the events considered. Fig. 4 shows the peak horizontal magnitude of velocity on the free surface for all events, and for the particular case of simulations done using the model CVM-S4.26. This figure illustrates how the basins in the

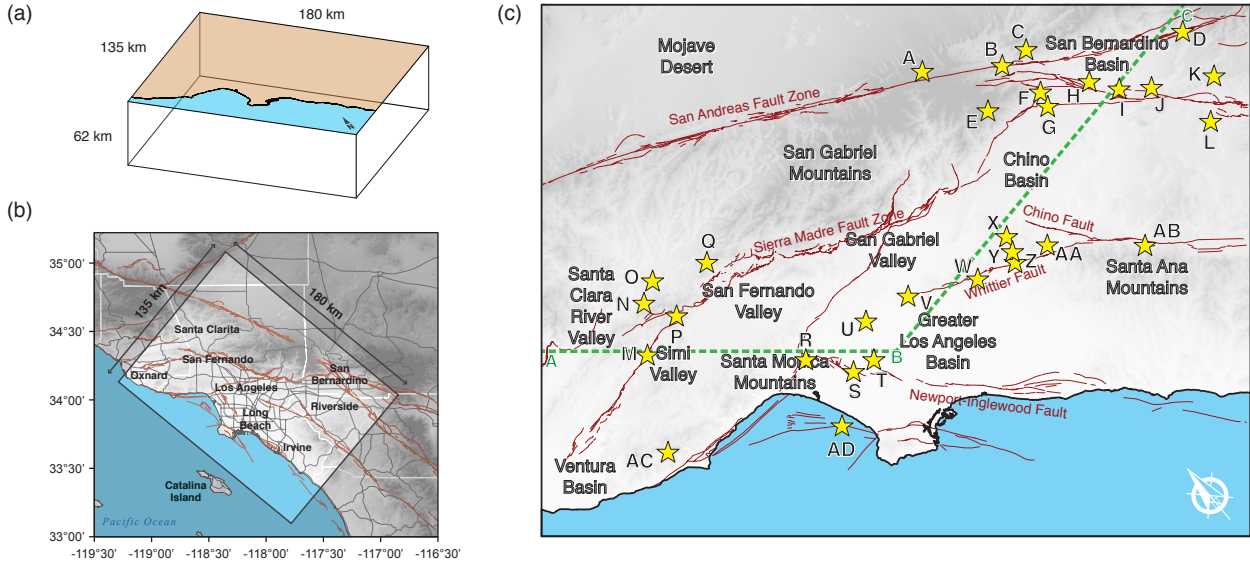


Figure 1. Region of interest and simulation domain. (a) 3D view of the simulation domain. (b) Geographical location and surface projection of the simulation domain, along with the names of the main cities surrounding the Los Angeles metropolitan area. (c) Major geologic structures including basins, valleys and mountains, along with the main quaternary faults in the region. The stars are representing the considered event in the area. The segments AB and BC are used as reference for Fig. 1.

Table 1. Selected events and description of source location, magnitude, focal mechanism,

Code	Earthquake name	Event ID	M_w	Coordinates (lon., lat.)	Depth (m)	Strike/Dip/Rake	Date (yyyy/mm/dd)	UTC Time (hh:mm:ss)	Num. Stns.
A	Wrightwood	9064568	4.40	-117.6480, 34.3740	8.99	285/57/86	1998/08/20	23:49:58.198	00
B	NW of Devore	10972299	3.79	-117.4642, 34.2655	10.91	98/58/68	2001/07/19	20:42:36.470	00
C	NNE of Devore	14494128	3.72	-117.3838, 34.2587	7.18	344/69/-33	2009/08/01	12:55:55.317	00
D	Yucaipa	14155260	4.88	-117.0113, 34.0580	11.61	75/59/55	2005/06/16	20:53:26.225	00
E	N of Rancho Cucamonga	10216101	3.60	-117.5762, 34.2058	4.92	54/69/16	2006/11/04	19:43:44.376	00
F	2002 Fontana	13692644	3.74	-117.4288, 34.1613	6.54	233/72/-28	2002/07/25	00:43:14.872	00
G	2005 Fontana	14116972	4.42	-117.4387, 34.1250	4.15	222/88/-25	2005/01/06	14:35:27.593	00
H	San Bernardino	10370141	4.45	-117.3042, 34.1073	14.22	87/70/28	2009/01/09	03:49:46.051	00
I	N of Loma Linda	9140050	4.37	-117.2525, 34.0500	15.36	270/90/-6	2000/02/21	13:49:43.017	00
J	Redlands	10541957	4.10	-117.1797, 34.0045	8.53	33/46/-68	2010/02/13	21:39:06.349	00
K	2010 Beaumont	10530013	4.28	-117.0232, 33.9322	13.93	234/89/9	2010/01/16	12:03:25.345	00
L	2006 Beaumont	14239184	3.90	-117.1122, 33.8560	11.53	45/31/-25	2006/07/10	02:54:43.809	00
M	Simi Valley	14000376	3.59	-118.7530, 34.2722	13.81	234/62/60	2003/10/29	23:44:48.206	00
N	WSW of Valencia	9753489	3.90	-118.6678, 34.3705	14.21	83/62/57	2002/01/29	06:00:39.140	00
O	N of Pico Canyon	9096972	3.98	-118.6090, 34.3980	11.53	287/55/54	1999/07/22	09:57:23.502	00
P	Chatsworth	14312160	4.66	-118.6195, 34.2995	7.58	82/27/51	2007/08/09	07:58:48.888	00
Q	Newhall	15237281	3.86	-118.4580, 34.3508	3.59	236/58/33	2012/10/28	15:24:23.172	00
R	Beverly Hills	9703873	4.24	-118.3885, 34.0590	7.90	262/81/4	2001/09/09	23:59:17.695	00
S	Inglewood Area	10410337	4.70	-118.3357, 33.9377	13.86	243/60/25	2009/05/18	03:39:36.126	00
T	NW of Compton	9716853	3.98	-118.2702, 33.9290	21.13	116/68/71	2001/10/28	16:27:45.388	00
U	Downtown Los Angeles	9093975	3.77	-118.2180, 34.0100	9.53	125/49/79	1999/06/29	12:55:00.371	00
V	Whittier Narrows	14601172	4.44	-118.0817, 33.9923	18.85	282/36/73	2010/03/16	11:04:00.026	00
W	La Habra	15481673	5.10	-117.9300, 33.9220	5.00	239/70/38	2014/03/29	04:09:42.970	00
X	Chino Hills	14383980	5.39	-117.7613, 33.9530	14.70	47/51/32	2008/07/29	18:42:15.960	00
Y	2002 Yorba Linda	9818433	4.75	-117.7758, 33.9173	12.92	34/84/-10	2002/09/03	07:08:51.675	00
Z	2009 Yorba Linda	10399889	3.98	-117.7892, 33.8940	4.23	208/65/26	2009/04/24	03:27:49.840	00
AA	ESE of Yorba Linda	9644101	3.64	-117.6882, 33.8777	3.59	56/65/37	2001/04/13	11:50:11.916	00
AB	Lake Elsinore	10275733	4.73	-117.4770, 33.7322	12.60	65/59/58	2007/09/02	17:29:14.827	00
AC	Westlake Village	10403777	4.42	-118.8825, 34.0667	14.17	254/73/30	2009/05/02	01:11:13.084	00
AD	Hermosa Beach	14738436	3.69	-118.4578, 33.8572	11.23	57/41/54	2010/06/07	23:59:27.165	00

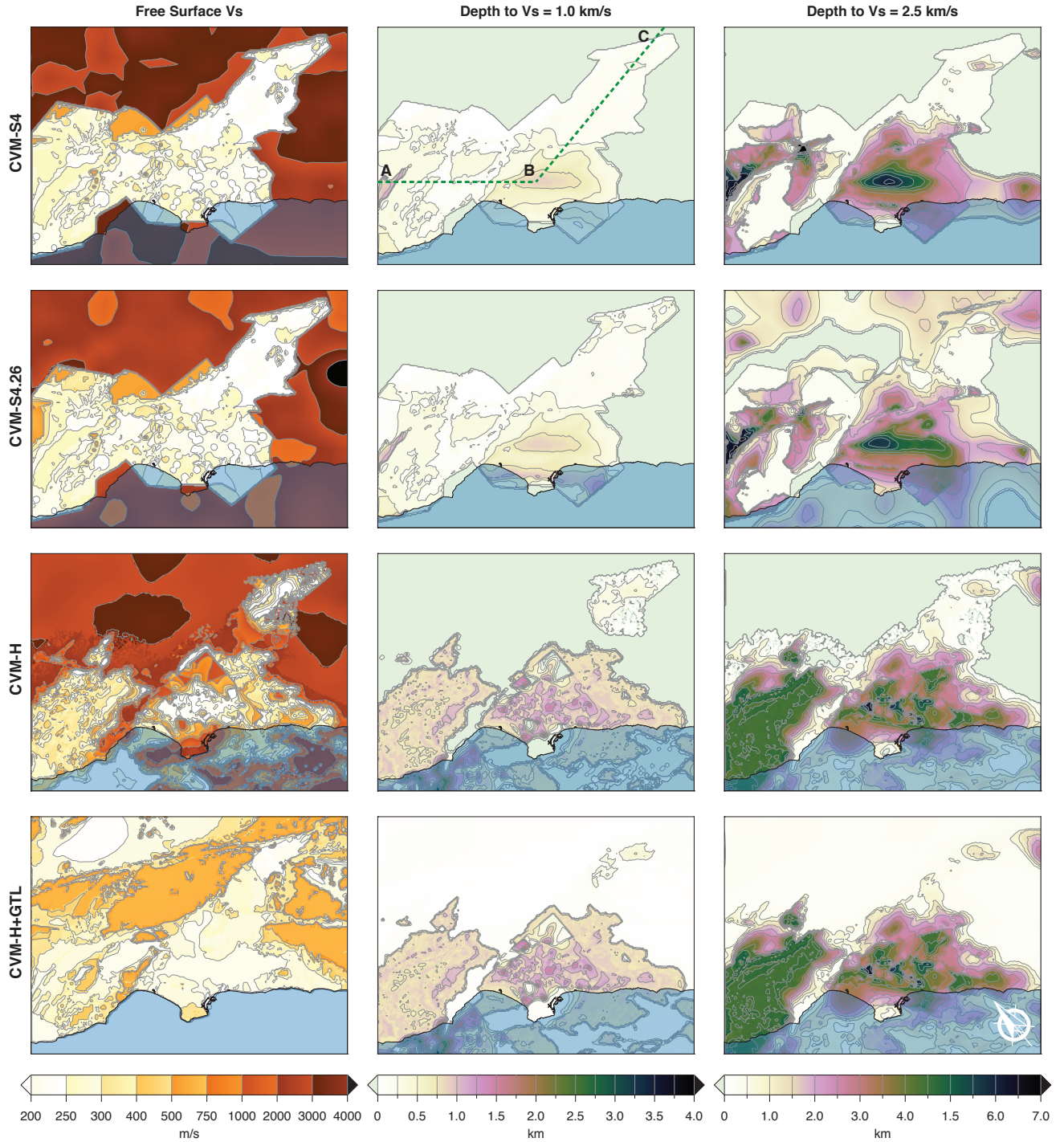


Figure 2. Comparison between the southern California community velocity models considered. Left: free-surface shear wave velocity, V_S . Center: depth to the isosurface at which $V_S = 1000$ m/s. Right: depth to the isosurface at which $V_S = 2500$ m/s.

region respond to earthquakes originated at various locations within the simulation domain. Although interpretations in this regard are biased by the choice of the color scale, it is fair to say that earthquakes of magnitude less than 3.9 remain local, showing only a marginal ground response in areas outside their immediate epicentral surrounding (e.g. events L, M, U). Events of magnitude greater than 4.3, on the other hand, show stronger response all throughout the domain, and exhibit more clearly the effects of the basins

(e.g. events D, P, Y). Events with magnitudes between 3.9 and 4.3 are in a transition zone. In such cases the shallower events register stronger ground motions (e.g. events Q and Z).

All events considered, the largest ground motions are obtained for the 2014 M_w 5.10 La Habra and 2008 M_w 5.39 Chino Hills earthquakes (events W and X, respectively), and the areas with most significant shaking are the greater Los Angeles basin, the San Bernardino basin and the region between Simi valley and the Ven-

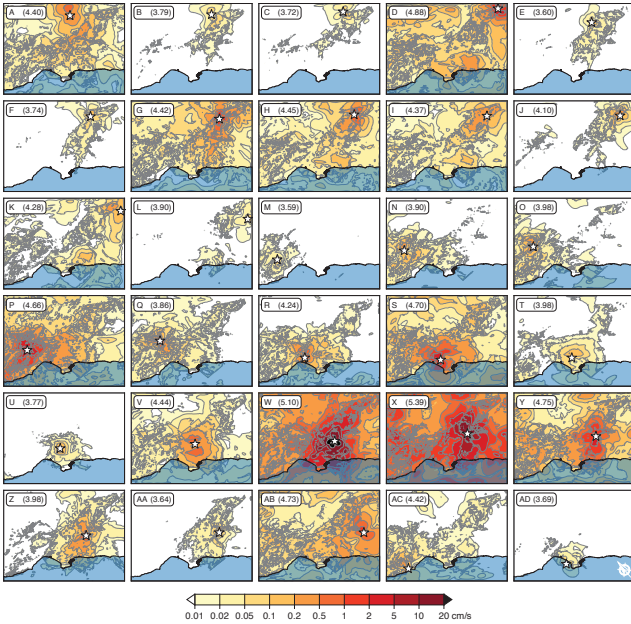


Figure 3. Source time functions (top: slip; middle: slip-rate), and slip-rate Fourier amplitude spectra (bottom) of all the events. Slip-rate functions were computed based on the total rise time estimated from eqs (??) and (??). The source functions of events W and X, corresponding to the 2014 La Habra and 2008 Chino Hills earthquakes, are singled out in the figure because for reference. These two events are the largest of all earthquakes considered.

Table 2. Simulation parameters and numerical model details.

Domain size	
Length (km)	180
Width (km)	135
Depth (km)	61.875
Domain corners ^a	
Southwest	-119.2888°, 34.120549°
Northwest	-118.3540°, 35.061096°
Northeast	-116.8460°, 34.025873°
Southeast	-117.7809°, 33.096503°
Numerical parameters	
f_{\max} (Hz)	1.0
V_S^{\min} (m/s)	200
Points/wavelength	8–15
Simulation Δt (s)	0.005
Simulation time (s)	100
Number of steps	20,000
Mesh details	
Min. element size (m)	21.97 m
Max. element size (m)	351.56 m
Number elements (mill.)	
CVM-S4	106.4
CVM-S4.26.2.2.1	110.3
CVM-S4.26.2.2.2	249.7
CVM-S4.26.2.2.3	282.6
Avg. simulation wall-clock time (hr:mm:ss) ^b	
CVM-S4	1:03:46
CVM-S4.26.2.2.1	1:03:58
CVM-S4.26.2.2.2	2:17:24
CVM-S4.26.2.2.3	2:40:51

^aThe corners of the domains are given in longitude and latitude.

^bCorresponding to 1,280 cores on NCSA's Blue Waters.

tura basin. While Fig. 4 only includes results obtained using CVM-S4.26, these observations are consistent across velocity models. We, however, now focus our attention to the discrepancies observed when using different velocity models.

Fig. 5 shows the peak horizontal magnitude of velocity on the free surface for all velocity models, for the particular cases of the 2005 M_w 4.42 Fontana, 2007 M_w 4.66 Chatsworth, and 2014 M_w 5.10 La Habra earthquakes (events G, P, and W, respectively). We select these three events for their location and magnitudes above 4, with well spread response over the simulation domain. The Fontana (G) earthquake epicenter was located in the northern section of the San Jacinto fault zone, not far from the junction with the San Andreas fault zone and the Cucamonga fault (see Fig. ??). This earthquake shows clear influence in the area of the San Bernardino basin for all four models, although with some differences. In the case of CVM-S4, for instance, a significant level of the response is channeled into the Chino and the greater Los Angeles basins, as well as far into the Simi and the Santa Clara river valleys. A similar response is seen in the case of CVM-S4.26, but to a lesser extend, with only marginal response in the Santa Monica area. CVM-S4.26 also exhibits lower values southwest and northwest from the epicenter than CVM-S4. In the cases of CVM-H and CVM-H+GTL, the ground motion is more localized around the epicentral area. Both models, however, seem to channel more energy along the north flank of the San Andreas Fault and to the south east and south west, in particular along the west edge of the Santa mountains, where both CVM-H and CVM-H+GTL have deeper structures than CVM-S4 or CVM-S4.26 (see Fig. 2 for reference).

In the case of the Chatsworth earthquake, the strongest response concentrates in the Simi and San Fernando valleys, along the Santa Clara river valley and into the Ventura basin. For the simulations done with CVM-S4 and CVM-S4.26, however, a greater amount of energy is channeled west into the Ventura basin and southeast towards the greater Los Angeles area. Both CVM-S4 and CVM-H show some level of basin effects in San Bernardino, an area where CVM-H+GTL shows the least level of amplification of all the models, due to the changes introduced by the GTL model as highlighted in Fig. ???. Both CVM-H and CVM-H+GTL show a stronger contrast between the Simi and San Fernando valleys and the Los Angeles basin, marked by the influence of the Santa Monica mountains, which seem to be more sharply defined in these two models than in CVM-S4 and CVM-S4.26 (see Fig. 2).

Last, in the case of the La Habra earthquake, the ground motions are mostly concentrated in the greater Los Angeles basin, though with some significant differences amongst the models. We first note again the fact that the model CVM-H+GTL introduces strong changes in the response of the San Bernardino basin with respect to CVM-H. As in other cases, CVM-H and CVM-H+GTL yield larger ground motions in the area of Irving (see Fig. 1) southeast from the epicenter. CVM-S4 and CVM-S4.26, on the other hand, exhibit larger ground motions within the Los Angeles basin itself and in the Chino basin. In turn, CVM-S4.26 yields larger shaking near the San Gabriel valley and mountains, and beyond in the Mojave desert. CVM-S4.26 also exhibits stronger response in the area of the Santa Ana mountains, as a result of the contrast in the model in this area with respect to CVM-S4. Of all four models, CVM-S4 has stronger response in the Ventura basin and CVM-H along the Santa Clara river valley—which likely reflects a better coupling between the crustal structure and faults representation in the model, considering the weak zone along the Santa Clara river due to the presence of the Oak Ridge fault beneath it.

Although not in equal measure for all events, the differences

Figure 4. Free surface peak horizontal magnitude velocity from simulations for all the events using the velocity model CVM-S4.26. The letter code used to identify each earthquake is shown at the top-left corner along with the event's magnitude, M_w (see Table 1). In each case, the star indicates the epicenter of the event (see also Fig. ??). Although smaller and larger values than those shown in the color scale were obtained from the simulations, these were truncated for visual convenience.

just highlighted were common among the models in the simulation results of other earthquakes. We further analyze the implications of these model discrepancies and their consequence in simulation results through the validation of synthetics against data in the following sections.

6 EVALUATION METHOD

We evaluate the accuracy of the simulations, and thus that of the velocity models, based on a quantitative validation of the simulated ground motions. The validation process consists of comparisons between synthetics and data, at locations where records were available for the simulated events. For this, we compiled a large collection of broadband and strong-motion records from two data centers, the Southern California Earthquake Data Center (SCEDC) and the Center for Engineering Strong Motion Data (CESMD). SCEDC and CESMD archive records from various seismic networks in the southern California region. In total we obtained records from more than 800 stations spread throughout the simulation domain. Unfortunately, not all the stations recorded all the events, thus the number of available data-points for comparisons varied between events. In addition, some stations were discarded for reasons explained below. The total number of stations with records used for validation is shown in Table 1 for each event.

Records from SCEDC and CESMD were processed and selected as follows. For each event, we first downloaded all the stations that recorded the earthquake and identified those that fell within the simulation domain boundaries. From this initial set, we kept only free-surface stations that free surface with records in three orthogonal components, two horizontal and one vertical. Although the majority of stations have instruments oriented as positive in the North (NS), East (EW), and up directions (UD), we rotated or sign-flipped those signals that had different orientations in order to bring them all to a common standard. Selecting only free-surface stations mean that we discarded stations from geotechnical arrays with stations at depth or stations that are part of structural monitoring arrays. In the case of strong ground motion records from CESMD, we preferred records that were available in their raw format (V1). For these records, whose original data correspond to accelerations, we performed gain and baseline corrections, and applied a **high-pass filter at 0.05 Hz** before integrating to obtain velocities and displacements. In the case of the records downloaded from SCEDC, we used both strong-motion accelerations (HN channels) or broadband velocities (BH channels). In general, we preferred HN channels, but used records from BH channels if these offered data not available in other formats. For HN channels, we proceeded similarly as we did with the V1 records from CESMD, high-pass filtering and integrating to obtain velocities and displacements. For BH channels, we derivate to obtain accelerations and high-pass filter and integrate the records to obtain displacements.

a complete set of displacement, velocity, and acceleration triplets in the N, EW, and Up signals to obtain the velocity and displacement time-series

ACKNOWLEDGMENTS

This work was supported by the United States Geological Survey (USGS) through the award “Evaluation of the southern California seismic velocity models through ground motion simulation and validation of past earthquakes” (G14AP00034); and by the Southern California Earthquake Center (SCEC) through the award “Evaluation of CVM-SI.26 perturbations integration involving undergraduate computer science and graduate earth sciences and engineering students” (14032). Additional support was provided through the U.S. National Science Foundation (NSF) award “SI2-SSI: A Sustainable Community Software Framework for Petascale Earthquake Modeling” (ACI-1148493). This research is also part of the Blue Waters sustained-petascale computing project, which is supported by NSF (awards OCI-0725070 and ACI-1238993) and the state of Illinois. Blue Waters is a joint effort of the University of Illinois at Urbana-Champaign and its National Center for Supercomputing Applications (NCSA). Computational support was possible through PRAC allocations supported by NSF awards “Petascale Research in Earthquake System Science on Blue Waters (PressOn-BlueWaters)” (ACI-0832698); and “Extending the spatiotemporal scales of physics-based seismic hazard analysis” (ACI-1440085). SCEC is funded by NSF Cooperative Agreement EAR-1033462 and USGS Cooperative Agreement G12AC20038. The SCEC contribution number for this paper is **PEDNING**.

REFERENCES

- Aagaard, B. T., Graves, R. W., Rodgers, A., Brocher, T. M., Simpson, R. W., Dreger, D., Petersson, N. A., Larsen, S. C., Ma, S., & Jachens, R. C., 2010. Ground-motion modeling of Hayward fault scenario earthquakes, Part II: Simulation of long-period and broadband ground motions, *Bull. Seismol. Soc. Am.*, **100**(6), 2945–2977.
- Anderson, J. G., 2004. Quantitative measure of the goodness-of-fit of synthetic seismograms, in *Proc. 13th World Conf. on Earthquake Eng.*, Int. Assoc. Earthquake Eng., Vancouver, British Columbia, Canada, Paper 243.
- Brocher, T. M., Aagaard, B. T., Simpson, R. W., & Jachens, R. C., 2006. The USGS 3D seismic velocity model for northern California, *Eos Trans. AGU*, **87**(52), Fall Meet. Suppl., Abstr. S51B–1266.
- Chaljub, E., Moczo, P., Tsuno, S., Bard, P.-Y., Kristek, J., Kaser, M., Stupazzini, M., & Kristekova, M., 2010. Quantitative comparison of four numerical predictions of 3D ground motion in the Grenoble Valley, France, *Bull. Seismol. Soc. Am.*, **100**(4), 1427–1455.
- Chen, P., Zhao, L., & Jordan, T. H., 2007. Full 3D tomography for the crustal structure of the Los Angeles region, *Bull. Seismol. Soc. Am.*, **97**(4), 1094–1120.
- Cui, Y., Olsen, K., Jordan, T., Lee, K., Zhou, J., Small, P., Roten, D., Ely, G., Panda, D., Chourasia, A., Levesque, J., Day, S., & Maechling, P., 2010. Scalable earthquake simulation on petascale supercomputers, in *SC '10: Proc. of the 2010 ACM/IEEE Int. Conf. for High Performance Computing, Networking, Storage and Analysis*, pp. 1–20.
- Fujiwara, H., Kawai, S., Aoi, S., Morikawa, N., Senna, S., Kudo, N., Ooi, M., Hao, K. X.-S., Hayakawa, Y., Toyama, N., Matsuyama, N., Iwamoto, K., Suzuki, H., & Ei, R., 2009. A study on subsurface structure model for deep sedimentary layers of Japan for strong-motion evaluation, Tech. Rep. 337, National Research Institute for Earth Science and Disaster Prevention, Tsukuba, Japan, (in Japanese).
- Gill, D., Small, P., Taborda, R., Lee, E.-J., Olsen, K. B., Maechling, P. J.,

Figure 5. Free surface peak horizontal magnitude velocity for three representative events (from top to bottom: G, W, and P) using all four velocity models (from left to right: CVM-S4, CVM-S4.26, CVM-H and CVM-H+GTL). The stars indicate the epicenter locations (see Table 1 and Fig. ?? for reference). In each case, smaller and larger values than those shown in the contour maps were obtained, but truncated for visual convenience.

- & Jordan, T. H., 2015. Standardized access to seismic velocity models using the unified community velocity model (UCVM) software, in *Abstr. SSA Annu. Meet.*, Pasadena, California, 21–23 April, Accepted.
- Graves, R., Jordan, T., Callaghan, S., Deelman, E., Field, E., Juve, G., Kesselman, C., Maechling, P., Mehta, G., Milner, K., Okaya, D., Small, P., & Vahia, K., 2011. CyberShake: A physics-based seismic hazard model for Southern California, *Pure Appl. Geophys.*, **168**(3–4), 367–381.
- Hauksson, E., 2000. Crustal structure and seismicity distribution adjacent to the Pacific and North America plate boundary in southern California, *J. Geophys. Res.*, **105**(B6), 13,875–13,904.
- Isbiliroglu, Y., Taborda, R., & Bielak, J., 2015. Coupled soil-structure interaction effects of building clusters during earthquakes, *Earthquake Spectra*, **31**(1), 463–500.
- Kohler, M. D., Magistrale, H., & Clayton, R. W., 2003. Mantle heterogeneities and the SCEC reference three-dimensional seismic velocity model version 3, *Bull. Seismol. Soc. Am.*, **93**(2), 757–774.
- Koketsu, K., Miyake, H., Fujiwara, H., & Tashimoto, T., 2008. Progress towards a Japan integrated velocity structure model and long-period ground motion hazard map, in *Proc. 14th World Conf. Earthquake Eng.*, no. S10-038, p. 7, October 12–17, Beijing, China.
- Lee, E.-J., Chen, P., Jordan, T. H., & Wang, L., 2011. Rapid full-wave centroid moment tensor (CMT) inversion in a three-dimensional earth structure model for earthquakes in Southern California, *Geophys. J. Int.*, **186**(1), 311–330.
- Lee, E.-J., Chen, P., & Jordan, T. H., 2014a. Testing waveform predictions of 3d velocity models against two recent los angeles earthquakes, *Seismol. Res. Lett.*, **85**(6), 1275–1284.
- Lee, E.-J., Chen, P., Jordan, T. H., Maechling, P. J., Denolle, M., & Beroza, G. C., 2014b. Full-3-D tomography for crustal structure in southern California based on the scattering-integral and the adjoint-wavefield methods, *J. Geophys. Res.*, **119**(8), 6421–6451.
- Magistrale, H., McLaughlin, K., & Day, S., 1996. A geology-based 3D velocity model of the Los Angeles basin sediments, *Bull. Seismol. Soc. Am.*, **86**(4), 1161–1166.
- Magistrale, H., Day, S., Clayton, R. W., & Graves, R., 2000. The SCEC southern California reference three-dimensional seismic velocity model version 2, *Bull. Seismol. Soc. Am.*, **90**(6B), S65–S76.
- Manakou, M. V., Raptakis, D. G., Chávez-García, F. J., Apostolidis, P. I., & Pitilakis, K. D., 2010. 3D soil structure of the Mygdonian basin for site response analysis, *Soil Dynam. Earthquake Eng.*, **30**(11), 1198–1211.
- Olsen, K. B., 1994. *Simulation of three-dimensional wave propagation in the Salt Lake basin*, Ph.D. thesis, University of Utah, Salt Lake City, Utah.
- Schlosser, S. W., Ryan, M. P., Taborda, R., López, J., O'Hallaron, D., & Bielak, J., 2008. Materialized community ground models for large-scale earthquake simulation, in *SC'08: Proc. ACM/IEEE Int. Conf. for High Performance Computing, Networking, Storage and Analysis*, p. 11, IEEE Computer Society, Austin, Texas.
- Small, P., Maechling, P., Jordan, T., Ely, G., & Taborda, R., 2011. SCEC UCVM — Unified California velocity model, in *Abstr. AGU Fall Meet.*, no. S21B-2200, San Francisco, California, December 5–9.
- Taborda, R. & Bielak, J., 2014. Ground-motion simulation and validation of the 2008 Chino Hills, California, earthquake using different velocity models, *Bull. Seismol. Soc. Am.*, **104**(4), 1876–1898.
- Taborda, R., López, J., O'Hallaron, D., Tu, T., & Bielak, J., 2007. A review of the current approach to CVM-Etrees, in *Proc. SCEC Annu. Meet.*, Palm Springs, CA, September 8–12.
- Taborda, R., López, J., Karaoglu, H., Urbanic, J., & Bielak, J., 2010. Speeding up finite element wave propagation for large-scale earthquake simulations, Tech. Rep. CMU-PDL-10-109, Carnegie Mellon University, Parallel Data Lab.
- Tromp, J., Tape, C., & Liu, Q., 2005. Seismic tomography, adjoint meth-
- ods, time reversal and banana-doughnut kernels, *Geophys. J. Int.*, **160**(1), 195–216.
- Tromp, J., Komatsitsch, D., Hjörleifsdóttir, V., Liu, Q., Zhu, H., Peter, D., Bozdag, E., McRitchie, D., Friberg, P., Trabant, C., & Hutko, A., 2010. Near real-time simulations of global cmt earthquakes, *Geophys. J. Int.*, **183**(1), 381–389.
- Tu, T., López, J., & O'Hallaron, D., 2003. The etree library: A system for manipulating large octrees on disk, Tech. Rep. CMU-CS-03-174, School of Computer Science, Carnegie Mellon University, Pittsburgh, Pennsylvania.
- Tu, T., Yu, H., Ramírez-Guzmán, L., Bielak, J., Ghattas, O., Ma, K.-L., & O'Hallaron, D. R., 2006. From mesh generation to scientific visualization: An end-to-end approach to parallel supercomputing, in *SC '06: Proc. ACM/IEEE Int. Conf. for High Performance Computing, Networking, Storage and Analysis*, p. 15, IEEE Computer Society, Tampa, Florida.
- Zhao, L., Jordan, T. H., Olsen, K. B., & Chen, P., 2006. Fréchet kernels for imaging regional earth structure based on three-dimensional reference models, *Bull. Seismol. Soc. Am.*, **95**(6), 2066–2080.